EUROPEAN JOURNAL OF COMPUTATIONAL MECHANICS
2018, VOL. 27, NO. 2, 89–108
https://doi.org/10.1080/17797179.2018.1469833

Taylor & Francis
Taylor & Francis Group

Check for updates

Numerical solution of time fractional partial differential equations using multiquadric quasi-interpolation scheme

M. Sarboland[a]

[a]Department of Mathematics, Saveh Branch, Islamic Azad University, Saveh, Iran

ABSTRACT

In this paper, a meshfree method is presented to solve time fractional partial differential equations. It is based on the multiquadric quasi-interpolation operator $\mathcal{L}_{\mathcal{W}_2}$. In the present scheme, quadrature formula is used to discretise the temporal Caputo fractional derivative of order $\alpha \in (0, 1]$ and the quasi-interpolation is used to approximate the solution function and its spatial derivatives. Our numerical results are compared with the exact solutions as well as the results obtained from the other numerical schemes. It can be easily seen that the proposed method is a reliable and effective method to solve fractional partial differential equation. Furthermore, the stability analysis of the method is surveyed.

ARTICLE HISTORY
Received 26 October 2017
Accepted 17 April 2018

KEYWORDS
Time fractional partial differential equation; multiquadric quasi-interpolation scheme

1. Introduction

In the last decade, fractional order partial differential equations are increasingly used to model problems in mathematical physics (Fan & Jiang, 2014; Qi & Jiang, 2011; Ray, 2015; Zhuang, Liu, Turner, & Gu, 2014), mathematics (Chen, Liu, Zhuang, & Anh, 2009; Feng, Zhuang, Liu, & Turner, 2015; Zhuang, Liu, Anh, & Turner, 2008), coloured noise (Sun, Abdelvahab, & Onaral, 1984), fluid and continuum mechanics (Carpinteri & Mainardi, 1997), finance (Sabatelli, Keating, Dudley, & Richmond, 2002; Song & Wang, 2013; Wyss, 2000) and biological processes and systems (Magin, Ingo, Colon-Perez, Triplett, & Mareci, 2013). Some of fractional partial differential equations (FPDEs) have been studied and solved, such as the time fractional nonlinear Sine-Gordon and Klein-Gordon equations (Dehghan, Abbaszadeh, & Mohebbi, 2015), the space fractional wave equation (Odibat and Momani, 2006), the time–space fractional telegraph equation (Momani, 2005; Orssingher & Beghin, 2004; Orssingher & Zhao, 2003; Zhao & Li, 2012), the fractional Fokker-Planck equation (Aminataei & Karimi Vanani, 2013; Chen, Liu, Zhuang, & Anh, 2009; Pinto & Sousa, 2017), the time–space fractional diffusion wave equation (Povstenko, 2010) and the fractional kdv equation (Debnath & Bhatta, 2004). Since most FPDEs do not have exact

CONTACT M. Sarboland m.sarboland@gmail.com

© 2018 Informa UK Limited, trading as Taylor & Francis Group

analytic solutions, so approximation and numerical methods are used extensively. Recently, the variational iterative method (Momani & Odibat, 2007), the Adomian decomposition method (El-Sayed & Gaber, 2006; Momani & Odibat, 2006) and radial basis function (RBF) meshless method (Uddin & Haq, 2011; Vanani & Aminataei, 2012) have been applied to solve such problems.

In the present work, we present a meshless approach for solving time FPDEs based on the multiquadric (MQ) quasi-interpolation operator $\mathcal{L}_{\mathcal{W}_2}$.

MQ quasi-interpolation is a linear combination of MQ-RBF and the approximated function. In 1992, (Beatson & Powell, 1992) proposed three univariate MQ quasi-interpolations named as $\mathcal{L}_A$, $\mathcal{L}_B$ and $\mathcal{L}_C$. (Wu & Schaback, 1994) presented the MQ quasi-interpolation $\mathcal{L}_D$. In recent years, (Jiang, Wang, Zhu, & Xu, 2011) have introduced a new MQ quasi-interpolation scheme. This approach is based on inverse multiquadric (IMQ) RBF interpolation, and Wu and Schaback's operator $\mathcal{L}_D$ that have the advantages of high approximation order. Up to now, MQ quasi-interpolation is applied for solving different types of PDEs, see (Jiang & Wang, 2012; Sarboland & Aminataei, 2014, 2015b, 2015a).

The outline of the present paper is as follows. A brief description of the MQ quasi-interpolation scheme is given in Section 2. In Section 3, we apply our numerical method for the time FPDEs. The stability analysis of the method is discussed in Section 4. The results of several numerical experiments are explained in Section 5. In Section 6, we conclude our results.

2. The MQ quasi-interpolation scheme

In this section, we describe three MQ quasi-interpolation schemes named as $\mathcal{L}_{\mathcal{D}}$, $\mathcal{L}_{\mathcal{W}}$ and $\mathcal{L}_{\mathcal{W}_2}$. More details can be seen in Beatson and Powell (1992), Jiang et al. (2011) and Wu and Schaback (1994).

For a given area $\Omega = [a, b]$ and a finite set of different points

$$a = x_0 < x_1 < \ldots < x_N = b, \quad h = \max_{1 \leqslant i \leqslant N} (x_i - x_{i-1}),$$

if we are supplied with a function $f : [a, b] \longrightarrow \mathbb{R}$, quasi-interpolation of f takes the form:

$$\mathcal{L}(f) = \sum_{i=0}^{N} f(x_i)\phi_i(x),$$

where each function $\phi_i(x)$ is a linear combination of the Hardy's MQs basis function (Hardy, 1971),

$$\psi_i(x) = \sqrt{c^2 + (x - x_i)^2},$$

and low-order polynomials and $c \in \mathbb{R}^+$ is a shape parameter. In Wu and Schaback (1994), Wu and Schaback introduced the MQ quasi-interpolation

operator $\mathcal{L}_{\mathcal{D}}$ that is defined as

$$\mathcal{L}_{\mathcal{D}} f(x) = \sum_{i=0}^{N} f(x_i)\widetilde{\psi}_i(x), \tag{1}$$

where

$$\widetilde{\psi}_0(x) = \frac{1}{2} + \frac{\psi_1(x) - (x - x_0)}{2(x_1 - x_0)},$$

$$\widetilde{\psi}_1(x) = \frac{\psi_2(x) - \psi_1(x)}{2(x_2 - x_1)} - \frac{\psi_1(x) - (x - x_0)}{2(x_1 - x_0)},$$

$$\widetilde{\psi}_i(x) = \frac{\psi_{i+1}(x) - \psi_i(x)}{2(x_{i+1} - x_i)} - \frac{\psi_i(x) - \psi_{i-1}(x)}{2(x_i - x_{i-1})}, \quad 2 \leqslant i \leqslant N - 2, \tag{2}$$

$$\widetilde{\psi}_{N-1}(x) = \frac{(x_N - x) - \psi_{N-1}(x)}{2(x_N - x_{N-1})} - \frac{\psi_{N-1}(x) - \psi_{N-2}(x)}{2(x_{N-1} - x_{N-2})},$$

$$\widetilde{\psi}_N(x) = \frac{1}{2} + \frac{\psi_{N-1}(x) - (x_N - x)}{2(x_N - x_{N-1})}.$$

Now, suppose that $\{x_{k_i}\}_{i=1}^{\bar{N}}$ is a smaller set of the given points $\{x_i\}_{i=0}^{N}$ where $\bar{N}$ is a positive integer satisfying $\bar{N} < N$ and $0 = k_0 < k_1 < \ldots < k_{\bar{N}+1} = N$. Using the IMQ-RBF, the second derivative of $f(x)$ can be approximated by RBF interpolant $S_{f''}$ as

$$S_{f''} = \sum_{j=1}^{\bar{N}} \alpha_j \bar{\varphi}(|x - x_{k_j}|),$$

where

$$\bar{\varphi}(r) = \frac{s^2}{(s^2 + r^2)^{3/2}},$$

and $s \in \mathbb{R}^+$ is a shape parameter.

The coefficients $\{\alpha_j\}_{j=1}^{\bar{N}}$ are uniquely obtained by the interpolation condition

$$S_{f''}(x_{k_i}) = \sum_{j=1}^{\bar{N}} \alpha_j \bar{\varphi}(|x_{k_i} - x_{k_j}|) = f''(x_{k_i}), \quad 1 \leqslant i \leqslant \bar{N}. \tag{3}$$

Since, the Equation (3) is solvable (Madych & Nelson, 1990), so

$$\alpha = A_X^{-1}.f_X'', \tag{4}$$

where

$$X = \{x_{k_1}, \ldots, x_{k_{\bar{N}}}\}, \quad \alpha = [\alpha_1, \ldots, \alpha_{\bar{N}}]^T, \quad A_X = [\bar{\varphi}(|x_{k_i} - x_{k_j}|)],$$
$$f_X'' = [f''(x_{k_1}), \ldots, f''(x_{k_{\bar{N}}})]^T.$$

Using the f and the coefficient α defined in Equation (4), a function $e(x)$ is constructed in the form

$$e(x) = f(x) - \sum_{j=1}^{\bar{N}} \alpha_j \sqrt{s^2 + (x - x_{k_j})^2}. \tag{5}$$

Now, using $\mathcal{L}_{\mathcal{D}}$ operator defined by Equation (1) on the data $\{(x_i, e(x_i))\}_{i=0}^{N}$ with the shape parameter c, the MQ quasi-interpolation operator $\mathcal{L}_{\mathcal{W}}$ is defined as follows:

$$\mathcal{L}_{\mathcal{W}} f(x) = \sum_{j=1}^{\bar{N}} \alpha_j \sqrt{s^2 + (x - x_{k_j})^2} + \mathcal{L}_{\mathcal{D}} e(x). \tag{6}$$

The shape parameters c and s should not be the same constant in Equation (6).

In Equation (3), the value of $f''_{x_{k_j}}$ can be replaced by

$$f''_{x_{k_j}} = \frac{2[(x_{k_j} - x_{k_j-1})f(x_{k_j+1}) - (x_{k_j+1} - x_{k_j-1})f(x_{k_j}) + (x_{k_j+1} - x_{k_j})f(x_{k_j-1})]}{(x_{k_j} - x_{k_j-1})(x_{k_j+1} - x_{k_j})(x_{k_j+1} - x_{k_j-1})},$$

when the data's $\{(x_{k_i}, f(x_{k_i}))\}_{i=1}^{\bar{N}}$ are given, and $\{x_i\}_{i=1}^{\bar{N}}$ aren't equally spaced points. So, if f_X'' in Equation (4) is replaced by

$$F_X'' = [f''_{x_{k_1}}, \ldots, f''_{x_{k_{\bar{N}}}}]^T, \tag{7}$$

the quasi-interpolation operator defined by Equations (5) and (6) is denoted by $\mathcal{L}_{\mathcal{W}_2}$. The linear reproducing property and the high convergence rate of $\mathcal{L}_{\mathcal{W}2}$ were also studied in Jiang et al. (2011).

The operator $\mathcal{L}_{\mathcal{W}_2}$ can be written in the compact form

$$\mathcal{L}_{\mathcal{W}_2} f(x) = \sum_{i=0}^{N} f(x_i)\widehat{\psi}_i(x), \tag{8}$$

where the basis functions $\widehat{\psi}_i(x)$ are a linear combination of functions $\widetilde{\psi}_i(x)$ and $\bar{\phi}_i(x) = \sqrt{s^2 + (x - x_i)^2}$. See Sarboland and Aminataei (2014) for details of compactness approach.

3. The numerical method

In this paper, we concentrate on the numerical solution of time fractional order partial differential equation of the type:

$$\frac{\partial^\alpha u(x,t)}{\partial t^\alpha} + \beta \frac{\partial u(x,t)}{\partial x} + \gamma \frac{\partial^2 u(x,t)}{\partial x^2} = f(x,t), \quad t \in [0,T], x \in \Omega = [a,b], 0 < \alpha \leq 1, \tag{9}$$

with the initial condition

$$u(x,0) = u_0(x), \tag{10}$$

and the boundary conditions,

$$u(a,t) = g_1(t), \qquad t \geq 0, \qquad u(b,t) = g_2(t), \tag{11}$$

where $u_0(x)$, $g_1(t)$, $g_2(t)$ and $f(x,t)$ are known functions, β and γ are real parameters, α is the order time derivative and $\frac{\partial^\alpha u(x,t)}{\partial t^\alpha}$ is the Caputo fractional partial derivative that defined as follows:

$$\frac{\partial^\alpha u(x,t)}{\partial t^\alpha} = \begin{cases} \frac{1}{\Gamma(1-\alpha)} \int_0^t \frac{\partial u(x,s)}{\partial s} (t-s)^{(-\alpha)} \mathrm{d}s, & 0 < t < T, 0 < \alpha < 1, \\ \frac{\partial u(x,t)}{\partial t}, & 0 \leq t \leq T, \alpha = 1, \end{cases} \tag{12}$$

where $\Gamma(.)$ is the Gamma function.

Now, we present the numerical scheme for solving the Equation (9) using the MQ quasi-interpolation $\mathcal{L}_{\mathcal{W}_2}$. In this approach, the quadrature formula is first employed for discretisation of the time fractional derivative similar to the work that has been done in Murio (2008). Then, the solution function is approximated by Equation (8), and their spatial derivatives are then obtained by symbolic differentiation. In the end, the collocation method is applied.

3.1. The discretisation of time fractional derivative

According to the simple quadrature formula see Murio (2008), the term $\frac{\partial^\alpha u(x,t_{n+1})}{\partial t^\alpha}$, $t_n = n\Delta t$ with step size Δt can be arranged as

$$\frac{\partial^\alpha u(x,t_{n+1})}{\partial t^\alpha} = a_\alpha \left[u^{n+1}(x) - u^n(x)\right] + a_\alpha \sum_{k=1}^{n} b_\alpha(k) \left[u^{n-k+1}(x) - u^{n-k}(x)\right] + O(\Delta t), \tag{13}$$

where $a_\alpha = \frac{(\Delta t)^{-\alpha}}{\Gamma(2-\alpha)}$, $b_\alpha(k) = (k+1)^{1-\alpha} - (k)^{1-\alpha}$ and $u^n(x) = u(x,t_n)$. See Murio (2008) for more details.

Substituting Equation (13) into Equation (9) yields the following time discretised form of the fractional differential equation:

$$a_\alpha \left[u^{n+1}(x) - u^n(x)\right] + a_\alpha \sum_{k=1}^{n} b_\alpha(k) \left[u^{n-k+1}(x) - u^{n-k}(x)\right] + \beta u_x^{n+1}(x) + \gamma u_{xx}^{n+1}(x) = f^{n+1}(x), \tag{14}$$

where $f^{n+1}(x) = f(x, t_{n+1})$.

Equation (14) can be written in the following form by some rearrangement of terms:

$$a_\alpha u^{n+1}(x) + \beta u_x^{n+1}(x) + \gamma u_{xx}^{n+1}(x) = a_\alpha u^n(x) + \chi^{n+1}(x), \tag{15}$$

where

$$\chi^{n+1}(x) = -a_\alpha \sum_{k=1}^{n} b_\alpha(k) \left[u^{n-k+1}(x) - u^{n-k}(x)\right] + f^{n+1}(x).$$

Now, the unknown function $u^n(x)$ is approximated using MQ quasi-interpolation scheme, and its spatial derivatives $u_x^n(x)$ and $u_{xx}^n(x)$ are calculated by differentiating such closed form quasi approximation as follows:

$$u^n(x) = \sum_{i=0}^{N} u_i^n \hat{\psi}_i(x), \tag{16}$$

$$u_x^n(x) = \sum_{i=0}^{N} u_i^n \frac{\partial \hat{\psi}_i}{\partial x}(x) = \sum_{i=0}^{N} u_i^n \check{\psi}_i(x), \tag{17}$$

$$u_{xx}^n(x) = \sum_{i=0}^{N} u_i^n \frac{\partial^2 \hat{\psi}_i}{\partial x^2}(x) = \sum_{i=0}^{N} u_i^n \bar{\psi}_i(x), \tag{18}$$

where $\frac{\partial \hat{\psi}_i}{\partial x} = \check{\psi}_i$ and $\frac{\partial^2 \hat{\psi}_i}{\partial x^2} = \bar{\psi}_i$.

At the end, replacing (16)-(18) into (15) and applying collocation method yields

$$\sum_{k=0}^{N} u_k^{n+1} \left[a_\alpha \hat{\psi}_{ik} + \beta \check{\psi}_{ik} + \gamma \bar{\psi}_{ik}\right] = a_\alpha \sum_{k=0}^{N} u_k^n \hat{\psi}_{ik} + \chi_i^{n+1}, \quad 1 \leqslant i \leqslant N-1, \tag{19}$$

where $\chi_i^{n+1} = \chi^{n+1}(x_i)$, $\hat{\psi}_{ik} = \hat{\psi}_k(x_i)$, $\check{\psi}_{ik} = \check{\psi}_k(x_i)$, and $\bar{\psi}_{ik} = \bar{\psi}_k(x_i)$, whereas according to (9):

$$u_0^n = u(x_0, t_n) = u(a, t_n) = g_1(t_n), \tag{20}$$

$$u_N^n = u(x_N, t_n) = u(b, t_n) = g_2(t_n). \tag{21}$$

Substituting (20) and (21) into (19) generates a system of $N-1$ linear equations in $N-1$ unknown parameters u_i^{n+1}.

Now, Equation (19) can be written in the matrix form

$$[a_\alpha \mathbf{A} + \beta \mathbf{D} + \gamma \ddot{\mathbf{D}}]\mathbf{u}^{n+1} = a_\alpha \mathbf{A}\mathbf{u}^n + \boldsymbol{\chi}^{n+1} + a_\alpha \sum_{k=0}^{1}\sum_{j=1}^{2} (-1)^k g_j^{n+k} \hat{\Psi}_j + \sum_{j=1}^{2} g_j^{n+1}[\beta \check{\Psi}_j + \gamma \bar{\Psi}_j], \tag{22}$$

where

$$\begin{aligned}
&\mathbf{A}_{ij} = [\hat{\psi}_{ij}]_{i,j=1}^{N-1}, \quad \mathbf{D}_{ij} = [\check{\psi}_{ij}]_{i,j=1}^{N-1}, \quad \ddot{\mathbf{D}}_{ij} = [\bar{\psi}_{ij}]_{i,j=1}^{N-1},\\
&\hat{\Psi}_1 = [\hat{\psi}_0(x_1), \hat{\psi}_0(x_2), \ldots, \hat{\psi}_0(x_{N-1})]^T,\\
&\hat{\Psi}_2 = [\hat{\psi}_N(x_1), \hat{\psi}_N(x_2), \ldots, \hat{\psi}_N(x_{N-1})]^T,\\
&\check{\Psi}_1 = [\check{\psi}_0(x_1), \check{\psi}_0(x_2), \ldots, \check{\psi}_0(x_{N-1})]^T,\\
&\check{\Psi}_2 = [\check{\psi}_N(x_1), \check{\psi}_N(x_2), \ldots, \check{\psi}_N(x_{N-1})]^T,\\
&\bar{\Psi}_1 = [\bar{\psi}_0(x_1), \bar{\psi}_0(x_2), \ldots, \bar{\psi}_0(x_{N-1})]^T,\\
&\bar{\Psi}_2 = [\bar{\psi}_N(x_1), \bar{\psi}_N(x_2), \ldots, \bar{\psi}_N(x_{N-1})]^T,
\end{aligned}$$

and

$$\boldsymbol{\chi}^{n+1} = [\chi^{n+1}(x_1), \chi^{n+1}(x_2), \ldots, \chi^{n+1}(x_{N-1})]^T.$$

Subsequently, Equation (22) can be written as

$$\mathbf{u}^{n+1} = \mathbf{M}^{-1}\mathbf{N}\mathbf{u}^n + \mathbf{M}^{-1}\Psi, \tag{23}$$

where

$$\begin{aligned}
&\mathbf{M} = a_\alpha \mathbf{A} + \beta \mathbf{D} + \gamma \ddot{\mathbf{D}}, \qquad \mathbf{N} = a_\alpha \mathbf{A},\\
&\boldsymbol{\Psi} = \boldsymbol{\chi}^{n+1} + a_\alpha \sum_{k=0}^{1}\sum_{j=1}^{2} (-1)^k g_j^{n+k} \hat{\Psi}_j + \sum_{j=1}^{2} g_j^{n+1}[\beta \check{\Psi}_j + \gamma \bar{\Psi}_j].
\end{aligned} \tag{24}$$

In order to make the reduction in error, the obtained u_i from (23) is substituted by Equation (16) that can be written as follows:

$$\mathbf{u}^n = \mathbf{A}\mathbf{u}^n + g_1^n \hat{\Psi}_1 + g_2^n \hat{\Psi}_2, \tag{25}$$

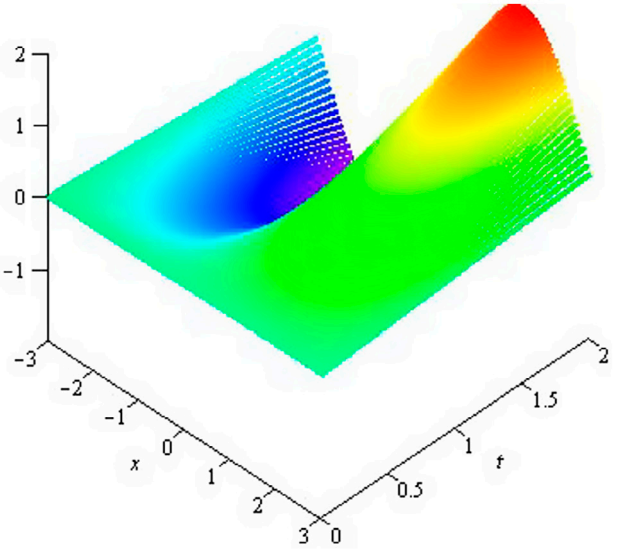

Figure 1. The space–time graph of estimated solution by MQQI for $x \in [0,1], t \in [0,2]$ and $\alpha = 0.6$ of experiment 1.

and the obtained value is considered as u_i. Therefore, it's taken from (23) and (25) that

$$\mathbf{u}^{n+1} = \mathbf{A}\,\mathbf{M}^{-1}\mathbf{N}\mathbf{A}^{-1}\mathbf{u}^n + \mathbf{A}\mathbf{M}^{-1}\Psi - \mathbf{A}\,\mathbf{M}^{-1}\mathbf{N}\mathbf{A}^{-1}(g_1^n\hat{\Psi}_1 + g_2^n\hat{\Psi}_2) + g_1^{n+1}\hat{\Psi}_1 + g_2^{n+1}\hat{\Psi}_2. \tag{26}$$

Hence, the unknown parameters u_i are specified from (26) instead of (23).

4. The stability analysis

In this section, the stability analysis of our numerical scheme is presented using spectral radius of the amplification matrix similar to the work that Islam et al. did in ul-Islam, Haq, and Uddin (2009). Let $\mathbf{u}^n$ be the exact and $\mathbf{u}^{*n}$ the numerical solution of Equation (9) at the nth time level, then the error ε^n at the nth time level is given by $\varepsilon^n = \mathbf{u}^n - \mathbf{u}^{*n}$. The error equation for discretised fractional partial differential equation can be written as

$$\varepsilon^{n+1} = \mathbf{A}\mathbf{M}^{-1}\mathbf{N}\mathbf{A}^{-1}\varepsilon^n = \mathbf{E}\,\varepsilon^n, \tag{27}$$

where $\mathbf{E} = \mathbf{A}\mathbf{M}^{-1}\mathbf{N}\mathbf{A}^{-1}$. It is noteworthy that this error includes both time and spatial errors at every time level. For the stability of the numerical scheme, we must have $\varepsilon^n \to 0$ as $n \to \infty$, i.e. $\rho(\mathbf{E}) \leqslant 1$, which is the necessary and sufficient condition for the numerical scheme to be stable, where $\rho(\mathbf{E})$ denotes the spectral radius of the amplification matrix $\mathbf{E}$. Equation (27) is equivalent with

$$\mathbf{M}\mathbf{A}^{-1}\varepsilon^{n+1} = \mathbf{N}\mathbf{A}^{-1}\varepsilon^n. \tag{28}$$

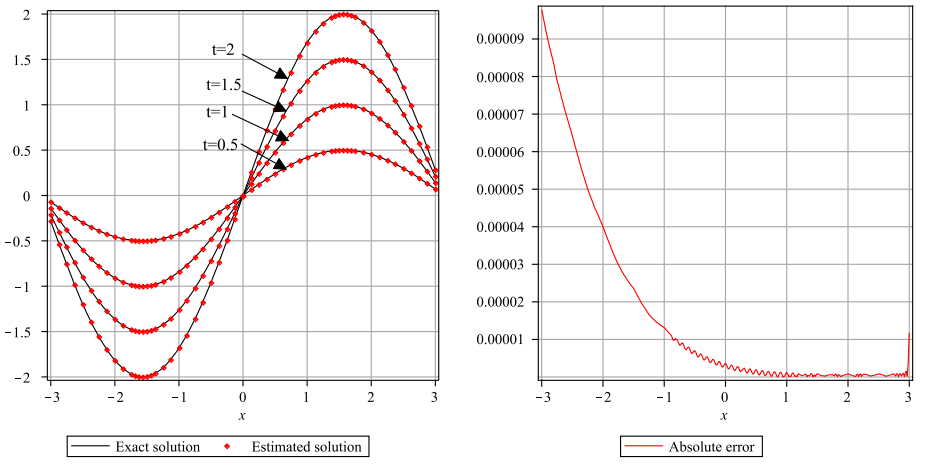

Figure 2. Absolute error and exact and estimated solutions at $t = 2$ with $\Delta t = 0.01$, $N = 121$ and $\alpha = 0.6$ of experiment 1.

Now, Equation (28) can be written into following form using the values of $\mathbf{M}$ and $\mathbf{N}$ defined in Equation (24):

$$[\mathbf{I} + (\Delta t)^{\alpha}\mathbf{R}]\varepsilon^{n+1} = \mathbf{I}\varepsilon^{n},$$

where

$$\mathbf{R} = c_{\alpha}[\beta\mathbf{D} + \gamma\ddot{\mathbf{D}}]\mathbf{A}^{-1}; \quad c_{\alpha} = \Gamma(2-\alpha).$$

The condition of stability will be satisfied if maximum eigenvalue of the matrix $\mathbf{E} = [\mathbf{I} + (\Delta t)^{\alpha}\mathbf{R}]^{-1}$ is less than or equal to unity, i.e.

$$\left|\frac{1}{1 + (\Delta t)^{\alpha}\eta_R}\right| \leqslant 1, \tag{29}$$

where η_R denotes the eigenvalue of the matrix $\mathbf{R}$. The above inequality holds true if either $\eta_R \geq 0$ or ($\eta_R \leq 0$ and $\Delta t \geq \sqrt[\alpha]{\frac{-2}{\eta_R}}$). It is clear that the condition number and magnitude of the eigenvalue of the matrix $\mathbf{R}$ depend on the shape parameter and the number of collocation points. Hence, the condition number and the spectral radius of the matrix $\mathbf{E}$ are dependent to the shape parameter and the number of collocation points. Since it is not possible to find explicit relationship among the spectral radius of the matrix and the shape parameter, this dependency is approximated numerically by keeping the number of collocation points fixed.

5. The numerical experiments

In this section, the proposed method is applied for five experiments. The numerical results of the FPDEs using this scheme are compared with the analytical solutions and solutions in Uddin and Haq (2011) (MQ scheme). Our numerical

scheme is denoted by MQQI. The L_∞ and L_2 error norms which are defined by

$$L_\infty = \|u^{*n} - u^n\|_\infty = \max_{0\leqslant j\leqslant N} |u^{*n}(x_j) - u^n(x_j)|,$$

$$L_2 = \|u^{*n} - u^n\|_2 = \sqrt{h\sum_{j=0}^{N}(u^{*n}(x_j) - u^n(x_j))^2},$$

are used to measure the accuracy. Also, the stability analysis of the methods is considered for first experiment. In all experiments, the shape parameter s is considered twice the shape parameter c.

The computations associated with the experiments discussed above were performed in Maple 16 on a PC with a CPU of 2.4 GHZ.

Experiment 1

Consider Equation (9) with the parameters $\beta = 1$, $\gamma = 0$ and the inhomogeneous term $f(x,t) = \frac{2t^{2-\alpha}}{\Gamma(2-\alpha)}\sin(x) + t\cos(x)$ that $\alpha = 0.6$. In this case, the FPDE (9) has the following form

$$\frac{\partial^\alpha u(x,t)}{\partial t^\alpha} + \frac{\partial u(x,t)}{\partial x} = \frac{2t^{2-\alpha}}{\Gamma(2-\alpha)}\sin(x) + t\cos(x), \tag{30}$$

that it's a one-dimensional linear inhomogeneous fractional wave equation.

The exact solution of (30) is given by $u(x,t) = t\sin(x)$ Odibat and Momani (2009). The initial condition in (10) and the boundary conditions in (11) can be obtained from the exact solution.

The results are presented for $\alpha = 0.6$ and compared with the exact solutions and the results of the MQ scheme Uddin and Haq (2011) in Table 1. In this case, we use the shape parameter $c = 0.09$, $\Delta t = 0.01$ and $N = 121$. It can be seen from Table 1 that the obtained results are in good agreement with the exact solutions and the results of the MQ scheme. We also compare the numerical solutions with the exact solution for various values of x at different times in Table 2.

Table 3 shows the relation between the spectral radius of the matrix E and the different values of the parameter c with fixed number collocation points $N = 50$ at $t = 0.5$. It is visible that if the values of shape parameter c are greater than the critical value $c = 0.18$, then $\rho(E) \geq 1$ and hence the MQQI method becomes unstable. Therefore, the interval stability of proposed scheme is $(0, 0.18)$ which is a small interval.

Moreover, the spatial rate of convergence obtained using our scheme are presented with $\Delta t = 0.01$ and different values of N at $t = 1$ in Table 4. It can be seen from Table 4 that the convergence rate increases with the smaller spatial step size and the error norms decrease. The time rate of convergence with $N = 40$ and different values of Δt is shown in Table 5. It is observable that the convergence rate decrease with a smaller time step size.

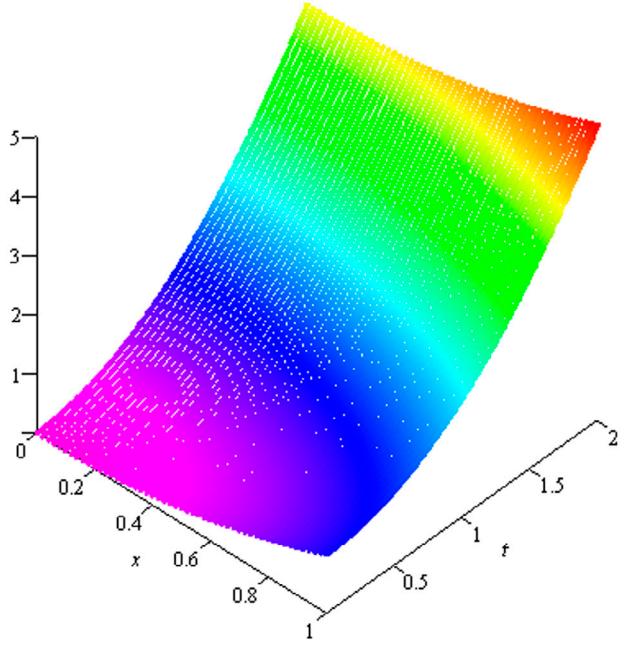

Figure 3. The space–time graph of estimated solution by MQQI for $x \in [0, 1], t \in [0, 2]$ and $\alpha = 0.5$ of experiment 2.

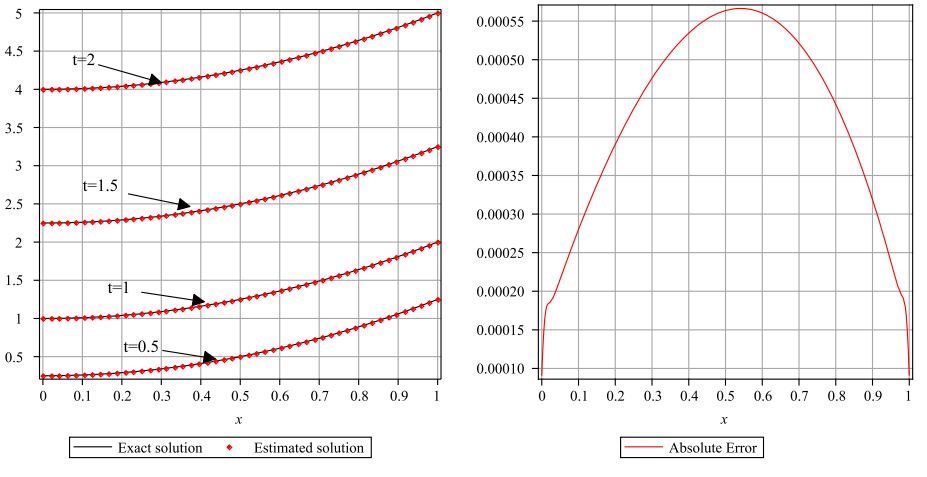

Figure 4. Absolute error and exact and estimated solutions at $t = 2$ with $\Delta t = 0.01, N = 51$ and $\alpha = 0.5$ of experiment 2.

The space–time plot of the estimated function is shown in Figure 1. Further, the graphs of absolute error and the estimated solution using our scheme are given at $t = 2$ in Figure 2.

Table 1. Comparison of the L_∞ and L_2 errors between the numerical results of our scheme and the results of Uddin and Haq (2011) with $\alpha = 0.6$, $\Delta t = 0.01$ and $N = 121$ at different times of experiment 1.

Time	0.1	0.5	1	1.5	2
MQQI;					
L_∞	3.13118E-06	1.80871E-05	4.23211E-05	6.93573E-05	9.78477E-05
L_2	1.11664E-06	9.68487E-06	2.67175E-05	4.86397E-05	7.47262E-05
MQ Uddin and Haq (2011);					
L_∞	1.152E-06	8.673E-06	1.894E-05	2.984E-05	4.070E-05
L_2	9.299E-07	1.730E-05	5.717E-05	1.142E-04	1.854E-04

Table 2. Comparison of results with the exact solution with $\alpha = 0.6$, $\Delta t = 0.01$ and $N = 121$ for different values of x and t of experiment 1.

x	0.5	1	1.5	2	2.5
$t = 0.5$					
Exact	0.23971	0.42074	0.49875	0.45465	0.29924
MQQI	0.23971	0.42074	0.49875	0.45465	0.29924
$t = 1$					
Exact	0.47943	0.84147	0.99750	0.90930	0.59847
MQQI	0.47943	0.84147	0.99749	0.90930	0.59847
$t = 1.5$					
Exact	0.71914	1.26221	1.49624	1.36395	0.89771
MQQI	0.71914	1.26221	1.49624	1.36395	0.89771
$t = 2$					
Exact	0.95885	1.68294	1.99499	1.81860	1.19694
MQQI	0.95885	1.68294	1.99499	1.81860	1.19694

Table 3. The spectral radius and L_∞ and L_2 error norms versus shape parameter c for $\Delta t = 0.01$ and $N = 50$ at $t = 0.5$ of experiment 1.

c	$\rho(\mathbf{E})$	L_∞	L_2
0.00001	0.99998	7.72317E-04	8.31526E-04
0.00010	0.99994	7.69874E-04	8.29521E-04
0.00100	0.99991	7.45230E-04	8.09243E-04
0.01000	0.99998	4.90979E-04	5.95721E-04
0.05000	1.00000	3.60981E-04	2.67189E-04
0.10000	1.00000	4.98564E-04	2.43980E-04
0.15000	1.00000	3.27169E-05	1.34562E-04
0.17000	0.99999	3.73084E-05	1.71903E-05
0.18000	2.18403	1.18919E+01	6.36746E-00

Table 4. The spatial rate of convergence at $t = 1$ with $\Delta t = 0.01$ of experiment 1.

N	L_∞	Order	L_2	Order
40	1.38814E-03	—	8.13572E-04	—
80	4.20181E-04	1.72406	2.23448E-04	1.86432
120	2.03546E-04	1.78755	1.04041E-04	1.88522
160	1.19899E-04	1.83965	6.00625E-05	1.90974
200	7.91060E-05	1.86368	3.90995E-05	1.92375

Table 5. The time rate of convergence at $t = 1$ with $N = 40$ of experiment 1.

Δt	L_∞	Order	L_2	Order
0.100	1.38864E-03	—	8.15129E-04	—
0.050	1.38829E-03	0.00026	8.14134E-04	0.00176
0.010	1.38814E-03	0.00007	8.13572E-04	0.00043
0.005	1.38813E-03	0.00002	8.13529E-04	0.00008
0.001	1.38812E-04	0.00001	8.13506E-04	0.00002

Table 6. The comparison of the L_∞ and L_2 errors of our method with the results of Uddin and Haq (2011) with $\alpha = 0.5$, $\Delta t = 0.01$ and $N = 51$ at different times of experiment 2.

Time	0.1	0.5	1	1.5	2
MQQI;					
L_∞	4.7807E-04	5.4079E-04	5.5630E-04	5.6368E-04	5.6897E-04
L_2	3.8201E-04	4.2643E-04	4.3724E-04	4.4260E-04	4.4654E-04
MQ Uddin and Haq (2011);					
L_∞	6.086E-02	2.958E-02	2.114E-02	1.732E-02	1.503E-02
L_2	2.613E-01	1.277E-01	9.134E-02	7.485E-01	6.494E-01

Experiment 2

In this experiment, we consider Equation (9) with $\beta = 1$, $\gamma = -1$, $[a, b] = [0, 1]$ and $f(x,t) = \frac{2t^{2-\alpha}}{\Gamma(3-\alpha)} + 2x - 2$, which is one-dimensional linear inhomogeneous fractional Burgers' equation Odibat and Momani (2009)

$$\frac{\partial^\alpha u(x,t)}{\partial t^\alpha} + \frac{\partial u(x,t)}{\partial x} - \frac{\partial^2 u(x,t)}{\partial x^2} = \frac{2t^{2-\alpha}}{\Gamma(3-\alpha)} + 2x - 2.$$

The exact solution of this experiment is

$$u(x,t) = x^2 + t^2. \tag{31}$$

The initial condition of the problem is obtained from (31) at $t = 0$ and the boundary conditions in (11) can be obtained from the exact solution.

Numerical results are listed for $\alpha = 0.5$ with $\Delta t = 0.01$ and compared with the results of Uddin and Haq (2011) in Table 6. Also, the numerical solutions are compared with the exact solutions for different values of x and t in Table 7. We use the shape parameter $c = 0.016$ with $N = 51$. Moreover, the space–time graph of the estimated solution is presented in Figure 3. Also, the graphs of absolute error and the estimated and analytical functions at $t = 2$ are shown in Figure 4.

Experiment 3

In this experiment, the Equation (9) is considered as the following form

$$\frac{\partial^\alpha u(x,t)}{\partial t^\alpha} = \frac{\partial^2 u(x,t)}{\partial x^2}, \tag{32}$$

with the initial condition

$$u(x,0) = 4x(1-x),$$

Table 7. Comparison of the results with the exact solutions with $\alpha = 0.5$, $\Delta t = 0.01$ and $N = 51$ for different values of x and t of experiment 2.

x	0.12	0.24	0.36	0.48	0.60	0.72	0.84	0.94
$t = 0.5$								
Exact	0.2644	0.3076	0.3796	0.4804	0.6100	0.7684	0.9556	1.1716
MQQI	0.2647	0.3080	0.3801	0.4809	0.6105	0.7689	0.9560	1.1718
$t = 1.0$								
Exact	1.0144	1.0576	1.1296	1.2304	1.3600	1.5184	1.7056	1.9216
MQQI	1.0147	1.0580	1.1301	1.2309	1.3605	1.5190	1.7060	1.9218
$t = 1.5$								
Exact	2.2644	2.3076	2.3796	2.4804	2.6100	2.7684	2.9556	3.1716
MQQI	2.2647	2.3080	2.3801	2.4810	2.6106	2.7689	2.9560	3.1718
$t = 2.0$								
Exact	4.0142	4.0576	4.1296	4.2304	4.3600	4.5184	4.7056	4.9216
MQQI	4.0147	4.0580	4.1301	4.2310	4.3606	4.5189	4.7060	4.9218

Table 8. The comparison of the L_∞ and L_2 errors of our method with $\Delta t = 0.01$, $c = 0.01$ and $N = 64$ at different times of experiment 4.

Time	0.2	0.4	0.6	0.8	1
$\alpha = 0.2$;					
L_∞	4.1337E-06	1.9913E-05	4.6348E-05	8.3447E-05	1.3125E-04
L_2	2.8311E-06	1.3469E-05	3.1316E-05	5.6361E-05	8.8643E-05
$\alpha = 0.5$;					
L_∞	6.2292E-06	1.5261E-05	3.5725E-05	7.2620E-05	1.2012E-04
L_2	4.8696E-05	7.4800E-06	2.4576E-05	4.9477E-05	8.1482E-05
$\alpha = 0.9$;					
L_∞	1.3344E-04	1.1983E-04	9.5632E-05	7.0402E-05	1.0225E-04
L_2	9.4744E-05	8.6462E-04	7.1672E-05	5.3182E-05	4.0570E-05

and the boundary conditions

$$u(0,t) = u(1,t) = 0.$$

The exact solution of Equation (32) is not known (Podlubny, Chechkin, Skovranek, Chen, & Jara, 2009). We have solved this problem by MQQI scheme with $N = 20$ and $\Delta t = 0.01$ for $\alpha = 1, 0.7$, and 0.5. The results are shown in Figure 5. This experiment is also solved by radial basis functions method (Uddin & Haq, 2011) and matrix approach (Podlubny et al., 2009). It should be observed that our results are very much identical with the results obtained in Podlubny et al. (2009) and Uddin and Haq (2011).

Experiment 4

In this experiment, we consider the time fractional diffusion equation

$$\frac{\partial^\alpha u(x,t)}{\partial t^\alpha} - \frac{\partial^2 u(x,t)}{\partial x^2} = \frac{2t^{2-\alpha}}{\Gamma(3-\alpha)} \sin(2\pi x) + 4\pi^2 t^2 \sin(2\pi x), \tag{33}$$

with the initial condition

$$u(x,0) = 0,$$

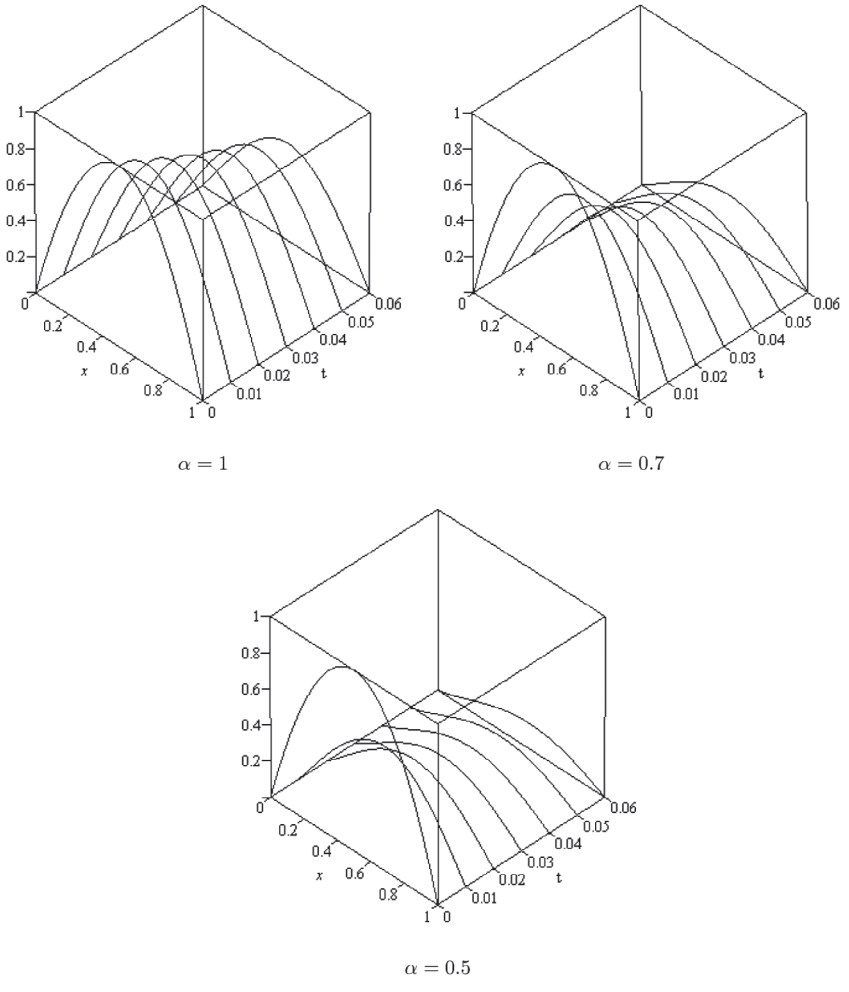

Figure 5. The space–time graph of estimated solution by MQQI for $x \in [0, 1], t \in [0, 0.06]$ and $\alpha = 1, 0.7$ and 0.5 of experiment 3.

and the boundary conditions

$$u(0, t) = u(1, t) = 0,$$

wherein $\beta = 0$, $\gamma = -1$, $[a, b] = [0, 1]$ and $f(x, t) = \frac{2t^{2-\alpha}}{\Gamma(3-\alpha)} \sin(2\pi x) + 4\pi^2 t^2 \sin(2\pi x)$.

The exact solution of this experiment is Li, Liang, and Yan (2017)

$$u(x, t) = t^2 \sin(2\pi x). \tag{34}$$

Numerical results of Equation (33) are obtained for $c = 0.016$ and $N = 64$ with $\Delta t = 0.01$. We have compared the exact solution and numerical solutions for our problem using values of $\alpha = 0.2$, $\alpha = 0.5$ and $\alpha = 0.9$ and tabulated in

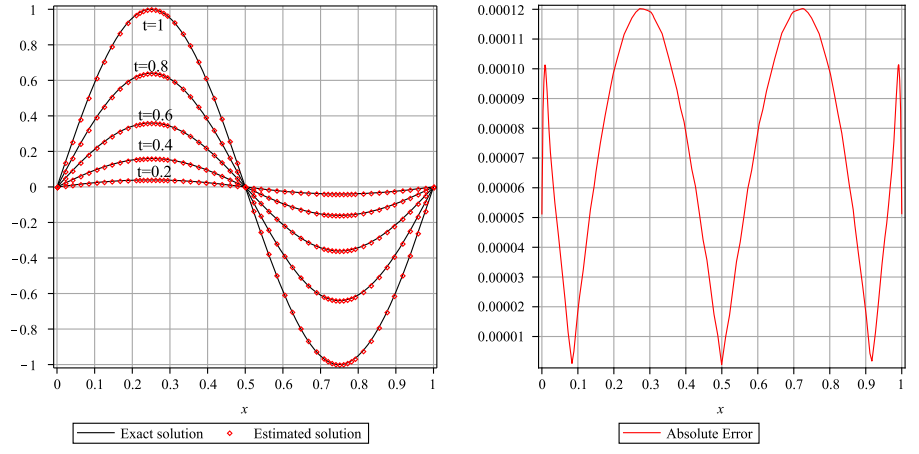

Figure 6. Absolute error and exact and estimated solutions with $\Delta t = 0.01, N = 64$ and $\alpha = 0.5$ of experiment 4.

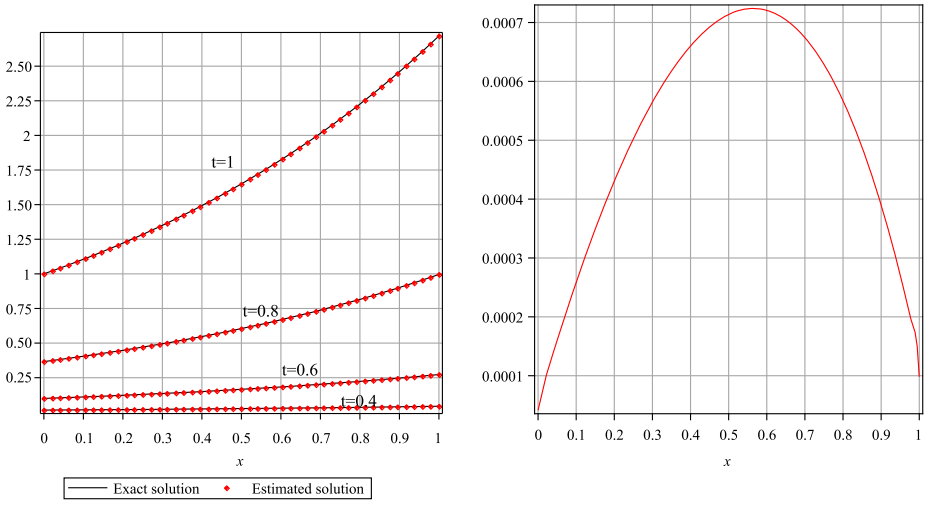

Figure 7. Absolute error and exact and estimated solutions with $\Delta t = 0.01, N = 64$ and $\alpha = 0.5$ of experiment 5.

Table 8. We can obviously see in this table that the exact and numerical solutions acquired by the scheme are in harmony with respect to each other.

Also, the graphs of approximate solutions acquired for $\alpha = 0.5$, $\Delta t = 0.01$ and $N = 64$ at various times have been illustrated in Figure 6.

Experiment 5

As a fifth experiment, we solve Equation (9) with $\beta = 0, \gamma = -1$ and $[a, b] = [0, 1]$ which is one-dimensional time fractional diffusion equation

$$\frac{\partial^\alpha u(x,t)}{\partial t^\alpha} - \frac{\partial^2 u(x,t)}{\partial x^2} = e^x \frac{\Gamma(5+\alpha)}{24} t^4 - t^{\alpha+4} e^x. \tag{35}$$

Table 9. The comparison of the L_∞ and L_2 errors of our method with $\Delta t = 0.01$, $c = 0.01$ and $N = 64$ at different times of experiment 5.

Time	0.2	0.4	0.6	0.8	1
$\alpha = 0.3$;					
L_∞	2.8296E-06	1.7079E-05	5.2127E-05	1.2224E-04	2.4844E-04
L_2	2.0883E-06	1.2818E-05	4.0039E-05	9.6229E-05	1.9984E-04
$\alpha = 0.5$;					
L_∞	8.5878E-06	5.7022E-05	1.7262E-04	3.8371E-04	7.2382E-04
L_2	6.3229E-06	4.2069E-05	1.3404E-04	2.8677E-04	5.4620E-04
$\alpha = 0.9$;					
L_∞	4.2865E-05	4.5074E-04	1.6991E-03	4.2690E-03	8.6414E-03
L_2	3.1956E-05	3.3319E-04	1.2517E-03	3.1406E-03	6.3535E-03

Table 10. Comparison of the results with the exact solutions with $\alpha = 0.5$, $\Delta t = 0.01$ and $N = 64$ for different values of x and t of experiment 5.

x	0.125	0.250	0.375	0.500	0.625	0.750	0.875
$t = 0.2$							
Exact	0.0008	0.0009	0.0010	0.0012	0.0013	0.0015	0.0017
MQQI	0.0008	0.0009	0.0010	0.0012	0.0013	0.0015	0.0017
$t = 0.4$							
Exact	0.0183	0.0208	0.0236	0.0267	0.0302	0.0343	0.0388
MQQI	0.0184	0.0208	0.0236	0.0268	0.0303	0.0343	0.0389
$t = 0.6$							
Exact	0.1138	0.1289	0.1461	0.1656	0.1875	0.2125	0.2408
MQQI	0.1138	0.1290	0.1462	0.1657	0.1877	0.2127	0.2409
$t = 0.8$							
Exact	0.4151	0.4704	0.5330	0.6040	0.6844	0.7756	0.8788
MQQI	0.4153	0.4707	0.5334	0.6044	0.6848	0.7759	0.8791
$t = 1.0$							
Exact	1.3315	1.2840	1.4550	1.6487	1.8682	2.1170	2.3989
MQQI	1.3315	1.2845	1.4556	1.6494	1.8689	2.1176	2.3993

The exact solution of this experiment is Li et al. (2017)

$$u(x,t) = e^x t^{\alpha+4}. \tag{36}$$

The initial condition in (10) and the boundary conditions in (11) can be obtained from the exact solution.

A comparison of the analytical and the obtained numerical solutions for values $\alpha = 0.3$, $\alpha = 0.5$ and $\alpha = 0.9$ has been given in Table 9. Also, the numerical solutions are compared with the exact solutions for different values of x and t in Table 10. It is clear in these tables that the approximate results are consistent with the theoretical results.

The graphs of absolute error and approximate solutions acquired for $\alpha = 0.5$, $\Delta t = 0.01$ and $N = 64$ at different times have been shown in Figure 7.

6. Conclusion

In this paper, a numerical scheme based on high accuracy MQ quasi-interpolation scheme and RBFs approximation scheme has been given for solving the time

fractional partial differential equations. The accuracy of the method can be improved by selecting the appropriate shape parameter.

The numerical results which are presented in the previous section demonstrate that the performance of the method is in excellent agreement with the exact solutions. Tables 1–10 show that the MQQI scheme is more accurate than MQ scheme in more cases.

It should be noted that in this paper, we used the univariate MQ quasi-interpolation scheme to solve the one-dimensional FPDEs, but this scheme can be extended and implemented for two-dimensional FPDEs similar work that we did in Sarboland and Aminataei (2015a). Besides, we use uniformly points in our numerical experiments, but our schemes can be used for the scattered points.

Disclosure statement

No potential conflict of interest was reported by the authors.

References

Aminataei, A., & Karimi Vanani, S. (2013). Numerical solution of fractional Fokker-Planck equation using the operational collocation method. *Applied and Computational Mathematics, 12*, 33–43.

Beatson, R. K., & Powell, M. J. D. (1992). Univariate multiquadric approximation: quasi-interpolation to scattered data. *Constructive Approximation, 8*, 275–288.

Carpinteri, A., & Mainardi, F. (1997). *Fractals and Fractional Calculus in Continuum Mechanics* (pp. 291–348). New York, NY: Springer-Verlag Wien.

Chen, S., Liu, F., Zhuang, P., & Anh, V. (2009). Finite difference approximations for the fractional Fokker-Planck equation. *Applied Mathematical Modelling, 33*, 256–273.

Debnath, L., & Bhatta, D. (2004). Solutions to few linear fractional inhomogeneous partial differential equations in fluid mechanics. *Fractional Calculus and Applied Analysis, 7*, 21–36.

Dehghan, M., Abbaszadeh, M., & Mohebbi, A. (2015). An implicit RBF meshless approach for solving the time fractional nonlinear Sine-Gordon and Klein-Gordon equations. *Engineering Analysis with Boundary Elements, 50*, 412–434.

El-Sayed, A. M. A., & Gaber, M. (2006). The Adomian decomposition method for solving partial differential equations of fractal order in finite domains. *Physics Letters A, 359*, 175–182.

Fan, W. P., & Jiang, X. Y. (2014). Parameters estimation for a one-dimensional time fractional thermal wave equation with fractional heat flux conditions. *Acta Physica Sinica -Chinese Edition, 63*, 140202–140230.

Feng, L. B., Zhuang, P., Liu, F., & Turner, I. (2015). Stability and convergence of a new finite volume method for a two-sided space-fractional diffusion equation. *Applied Mathematics and Computation, 257*, 52–65.

Jiang, Z. W., Wang, R. H., Zhu, C. G., & Xu, M. (2011). High accuracy multiquadric quasi-interpolation. *Applied Mathematical Modelling, 35*, 2185–2219.

Jiang, Z. W., & Wang, R. H. (2012). Numerical solution of one-dimensional Sine-Gordon equation using high accuracy multiquadric quasi-interpolation. *Applied Mathematics and Computation, 218*, 7711–7716.

Hardy, R. L. (1971). Multiquadric equations of topography and other irregular surfaces. *Journal of Geophysical Research, 176*, 1905–1915.

Li, Z., Liang, Z., & Yan, Y. (2017). High-order numerical method for solving time fractional partial differential equation. *Journal of Scientific Computing*, *71*, 785–803.

Madych, W. R., & Nelson, S. A. (1990). Multivariate interpolation and conditionally positive definite functions. *Mathematics of Computation, 54*, 211–230.

Magin, R. L., Ingo, C., Colon-Perez, L., Triplett, W., & Mareci, T. H. (2013). Characterization of anomalous diffusion in porous biological tissues using fractional order derivatives and entropy. *Microporous and Mesoporous Materials, 178*, 39–43.

Momani, S. (2005). Analytic and approximate solutions of the space and time fractional telegraph equations. *Applied Mathematics and Computation, 170*, 1126–1134.

Momani, S., & Odibat, Z. (2006). Analytical solution of a time-fractional Navier-Stokes equation by Adomian decomposition method. *Applied Mathematics and Computation, 177*, 488–494.

Momani, S., & Odibat, Z. (2007). Comparison between the homotopy perturbation method and the variational iteration method for linear fractional partial differential equations. *Computers and Mathematics with Applications, 54*, 910–919.

Murio, D. A. (2008). Implicit finite difference approximation for time fractional diffusion equations. *Computers and Mathematics with Applications, 56*, 1138–1145.

Odibat, Z. M., & Momani, S. (2006). Approximate solutions for boundary value problems of time-fractional wave equation. *Applied Mathematics and Computation, 181*, 767–774.

Odibat, Z. M., & Momani, S. (2009). The variational iteration method: an efficient scheme for handling fractional partial differential equations in fluid mechanics. *Computers and Mathematics with Applications, 58*, 2199–2208.

Orssingher, E., & Beghin, L. (2004). Time fractional telegraph equation and telegraph process with brownian time. *Probability Theory and Related Fields, 128*, 141–160.

Orssingher, E., & Zhao, X. (2003). The space fractional telegraph equation and the related telegraph process. *Chinese Annals of Mathematics, 24B*, 45–56.

Pinto, L., & Sousa, E. (2017). Numerical solution of a time-space fractional Fokker-Planck equation with variable force field and diffusion. *Commm. Nonlinear Science and Numerical Simulation, 50*, 211–228.

Podlubny, I., Chechkin, A., Skovranek, T., Chen, Y., & Jara, B. (2009). Matrix approach to discrete fractional calculas II: Partial fractional differential equation. *Journal of Computational Physics, 228*, 3137–3153.

Povstenko, Y. Z. (2010). Evolution of the initial box-signal for time-fractional diffusion-wave equation in a case of different spatial dimensions. *Physics A, 389*, 4696–4707.

Qi, H., & Jiang, X. (2011). Solutions of the space-time fractional Cattaneo diffusion equation. *Physics A, 390*, 1876–1883.

Ray, S. S. (2015). Two reliable approaches involving haar wavelet method and optimal homotopy asymptotic method for the solution of fractional fisher type equation. *Journal of Physics: Conference Series, 574*, 112–131.

Sabatelli, L., Keating, S., Dudley, J., & Richmond, P. (2002). Waiting time distributions in financial markets. *European Physical Journal B, 27*, 273–275.

Sarboland, M., & Aminataei, A. (2014). On the numerical solution of one-dimensional nonlinear nonhomogeneous Burgers' equation. *Journal of Applied Mathematics*, *2014*, Article ID 598432, 15.

Sarboland, M., & Aminataei, A. (2015a). An efficient numerical scheme for coupled nonlinear Burgers' equations. *Applied Mathematics and Information Sciences, 1*, 245–255.

Sarboland, M., & Aminataei, A. (2015b). On the numerical solution of the nonlinear Korteweg-de Vries equation. *Systems Science and Control Engineering, 3*, 69–80.

Song, L., & Wang, W. (2013). Solution of the fractional Black-Scholes option pricing model by finite difference method. *Abstract and Applied Analysis, 45*, 1–16.

Sun, H. H., Abdelvahab, A. A., & Onaral, B. (1984). Linear approximation of transfer function with a pole of fractional order. *IEEE Transactions on Automatic Control, 29*, 441–444.

Uddin, M., & Haq, S. (2011). RBFs approximation method for time fractional partial differential equations. *Communications in Nonlinear Science and Numerical Simulation, 16*, 4208–4214.

ul-Islam, S., Haq, S., & Uddin, M. (2009). A meshfree interpolation method for the numerical solution of the coupled nonlinear partial differential equations. *Engineering Analysis with Boundary Elements*, *33*, 399–409.

Vanani, S. K., & Aminataei, A. (2012). On the numerical solution of fractional partial differential equations. *Mathematical and Computational Applications, 17*, 140–151.

Wu, Z. M., & Schaback, R. (1994). Shape preserving properties and convergence of univariate multiquadric quasi- interpolation. *Acta Mathematicae Applicatae Sinica (English Ser.), 10*, 441–446.

Wyss, W. (2000). The fractional Black-Scholes equation. *Fractional Calculus and Applied Analysis, 3*, 51–61.

Zhao, Z., & Li, C. (2012). Fractional difference/finite element approximations for the time-space fractional telegraph equation. *Applied Mathematics and Computation, 219*, 2975–2988.

Zhuang, P., Liu, F., Turner, I., & Gu, Y. T. (2014). Finite volume and finite element methods for solving a one-dimensional space-fractional Boussinesq equation. *Applied Mathematical Modelling, 38*, 3860–3870.

Zhuang, P., Liu, F., Anh, V., & Turner, I. (2008). New solution and analytical techniques of the implicit numerical method for the anomalous subdiffusion equation. *SIAM Journal on Numerical Analysis, 46*, 1079–1095.